

Frequency Dependence of Shot Noise in a Diffusive Mesoscopic Conductor

R. J. Schoelkopf, P. J. Burke, A. A. Kozhevnikov, and D. E. Prober

Departments of Applied Physics and Physics, Yale University, New Haven, Connecticut 06520-8284

M. J. Rooks

Cornell Nanofabrication Facility, Knight Laboratory, Cornell University, Ithaca, New York 14853

(Received 22 November 1996)

Detailed measurements of the voltage, temperature, and frequency dependence of the nonequilibrium current fluctuations for a diffusive mesoscopic conductor are reported. The data confirm predictions that a mesoscopic conductor shorter than the electron-electron inelastic length will display shot noise. Furthermore, the low temperatures (100 mK) and high frequencies (1–20 GHz) used for the measurements allow tests in the high-frequency regime (i.e., $h\nu \gg eV$ and kT) of the shot noise, which clearly show the influence of vacuum fluctuations. The quantum noise causes a high-frequency “cutoff” in the shot noise, i.e., the noise is independent of bias voltage for frequencies $\nu > eV/h$. [S0031-9007(97)02944-X]

PACS numbers: 73.23.Ps, 05.40.+j, 42.50.Lc, 72.70.+m

Is shot noise “white?” Shot noise occurs in a wide variety of systems [1], due to the passage of individual electrons from one side of the device to the other. If the current I is indeed composed of completely uncorrelated, discrete “shots” of charge e , then the current spectral density of the fluctuations is given by the well-known Poisson limit $S_I(\nu) = 2eI$ and is independent of frequency, i.e., white. At sufficiently high frequencies, however, this relation must break down. A correct treatment of the high-frequency spectrum of shot noise should include the details of correlations among the electrons which could arise due to Coulomb interactions and the Pauli exclusion principle, and should also include vacuum (zero-point) fluctuations. In fact, measurements of the shot noise spectrum should shed light on the detailed physics of electron transport in the system under study.

Recently, much attention has been focused on shot noise in mesoscopic systems, in which the electron transport is phase coherent. Measurements of the shot noise in ballistic mesoscopic conductors, such as quantum point contacts [2–4], have shown that the overall level of the shot noise is reduced when the transmission of the quantum channels is large, as predicted by Khlus and by Lesovik [5,6]. Shot noise in a diffusive mesoscopic conductor shorter than the inelastic electron-electron length L_{ee} was predicted [7,8] to have a reduced magnitude of $S_I = 2eI/3$, since even in the presence of large amounts of elastic scattering, there are a significant number of channels with large transmission probability. For a longer conductor with $L_{ee} < L < L_{eph}$, Steinbach *et al.* [9] measured the noise due to electron self-heating. They observed a crossover toward suppressed shot noise for $L \ll L_{ee}$. In this Letter, we present the first high-frequency measurements of the nonequilibrium current fluctuations of a diffusive mesoscopic conductor. Furthermore, these measurements represent the first direct, systematic tests of the frequency spectrum of electron shot

noise for any system in the high-frequency regime, where $h\nu$ is greater than either eV or kT .

The frequency spectrum of the current fluctuations in a quantum point contact was derived by Yang [10]. Büttiker calculated the noise of a phase-coherent conductor (i.e., $L < L_{ee}$) with multiple conducting channels, including the possibility of energy-dependent scattering [11]. In the simplest case of a two-terminal conductor with energy-independent transmission, the current spectral density reduces to

$$S_I(\nu) = \sum_n^N D_n(1 - D_n) \frac{2e^2}{h} \left\{ (eV + h\nu) \times \coth \left[\frac{eV + h\nu}{2kT} \right] + (eV - h\nu) \times \coth \left[\frac{eV - h\nu}{2kT} \right] \right\} + \sum_n^N D_n^2 \frac{2e^2}{h} \left\{ 2h\nu \coth \left[\frac{h\nu}{2kT} \right] \right\}, \quad (1)$$

where N is the number of conducting modes, each with transmission probability D_n , and T is the temperature of the electron reservoirs on either side of the constriction. The prefactor of the first term expresses the suppression of shot noise due to the Fermi statistics of the charge carriers. The last term gives the correct fluctuations at equilibrium (i.e., at $V = 0$). Note that in the limit that all the D_n are small, Eq. (1) reduces to the form derived [12] for a tunnel junction.

The current spectral density given in Eq. (1) reduces to more familiar forms in several limiting cases. When $eV \gg kT$ and $h\nu$, it yields shot noise with $S_I = \eta 2eI$. Here η is the suppression factor $\eta = \sum D_n(1 - D_n) / \sum D_n$. This factor is predicted [7] to be 1/3 for the diffusive case with $L < L_{ee}$. The equilibrium fluctuations (i.e., at zero voltage) are given by $S_I = 2h\nu G \coth[h\nu/2kT]$, where G is the

total conductance $G = \frac{2e^2}{h} \sum D_n$, in agreement with the fluctuation-dissipation theorem [13]. Thus for low frequencies and low biases ($eV \ll kT$), we recover the well-known Johnson noise limit $S_I = 4kTG$. Finally, in the limit where $h\nu \gg eV$ and kT , the noise is dominated by vacuum fluctuations or “quantum noise,” with $S_I = 2h\nu G$. While it may be tempting to picture Eq. (1) as representing a simple sum of these three different noise processes, they are in fact intimately related, and Eq. (1) represents a *nonlinear superposition* of Johnson, shot, and quantum noises.

The unusual nature of this superposition can be emphasized by examining the fluctuations predicted by Eq. (1) as a function of voltage for different frequencies (see Fig. 1). At zero frequency (full line), there is a transition from Johnson noise to the linearly rising shot noise at $eV \sim kT$ ($\sim 2 \mu\text{eV}$). At 20 GHz (dotted line), the fluctuations are dominated by quantum noise and do *not* increase from their equilibrium value until the voltage $V_{\text{cutoff}} = h\nu/e$ is exceeded, even though the condition $eV > kT$ is fulfilled and the low-frequency fluctuations (solid line) are increasing rapidly. This plateau at high frequencies occurs because the transmission of electrons in each channel is correlated [14] in time, and roughly periodic at the “attempt frequency” $\nu = eV/h$. Alternatively, an observation of voltage-independent noise for $|V| < V_{\text{cutoff}}$ can be viewed as confirmation of the

frequency-dependent fluctuation-dissipation theorem in this mesoscopic resistor. The vacuum contribution to the *equilibrium* fluctuations was measured previously in a resistor [15] and in the resistive termination of a waveguide [16]. In addition, noise temperatures limited by quantum fluctuations have been observed [17] in mixers based on superconducting tunnel junctions. However, the crossover from vacuum fluctuations to shot noise at nonzero bias (i.e., not at equilibrium) has, to our knowledge, not yet been observed in any system.

To investigate this spectral dependence of the shot noise, we performed high-frequency measurements of fluctuations in a diffusive metallic film shorter than the electron-electron inelastic length. The sample consisted of a thin (10 nm) gold film patterned via *e*-beam lithography into a strip 40 nm wide by 200 nm long. The gold film had a diffusion constant of about $40 \text{ cm}^2/\text{s}$ and a nearly temperature-independent sheet resistance of $9 \Omega/\text{square}$. The length of the strip was defined by a pair of thick (80 nm) clean Au contacts, which have a sheet resistance of less than $0.1 \Omega/\text{square}$. Below 1 K, the predominant phase-breaking mechanism is electron-electron scattering. Based on the known diffusion constant and resistivity, we calculate [18] that the electron-electron inelastic length L_{ee} should be greater than $2 \mu\text{m}$ at 100 mK, so that $L \ll L_{ee}$ for all the measurements described here.

This device was cooled to less than 100 mK in a dilution refrigerator and coupled to a cryogenically cooled, broadband HEMT amplifier covering the frequency range 1–20 GHz. The high frequencies used avoid complications due to $1/f$ noise and allow access to the high-frequency regime, since $h\nu/kT \sim 10$ at 20 GHz and 100 mK. In order to observe noise levels on the order of mK while the amplifier contribution is about 100 K, we apply a low-frequency modulation to the bias voltage on the device and detect the synchronous change in amplifier output power in a broad bandwidth $B \sim 0.5 \text{ GHz}$. As shown in Fig. 2, the experimental configuration allowed for simultaneous measurement in two frequency bands, at a low frequency (1.5 GHz) and at a high frequency between 5 and 20 GHz. The combination of broad measurement band, good impedance matching to the device (with $R \sim 47\Omega$), and synchronous detection allows very sensitive measurements of the change in the noise

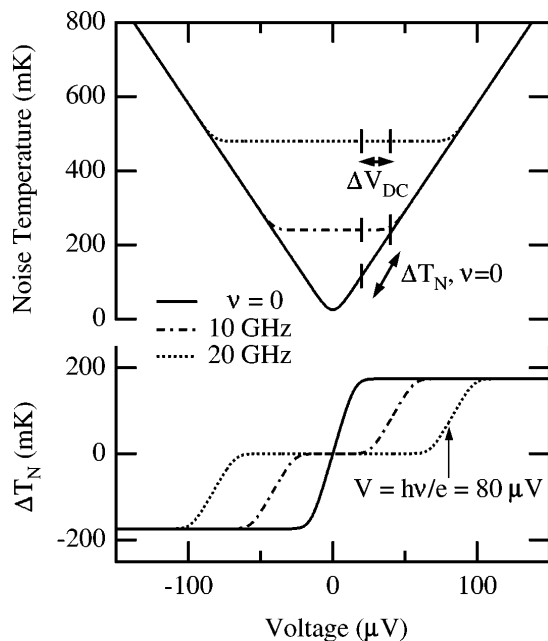


FIG. 1. Predicted dc bias voltage dependence of noise (top) for three frequencies at a bath temperature of 25 mK. The current spectral density predicted by Eq. (1), with $D_n \ll 1$ for all n , has been converted to an equivalent noise temperature T_N through the relation $T_N = S_I/4kG$. Note that the noise is *independent* of bias voltage for $e|V| < h\nu$. The bias voltage modulation technique is shown schematically and the expected differential noise ΔT_N for a $30 \mu\text{V}$ p.p. modulation is also displayed (bottom).

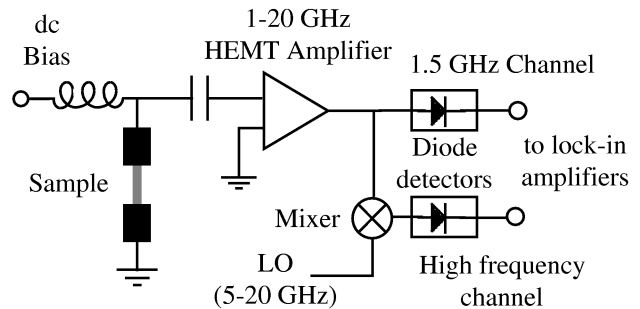


FIG. 2. Schematic of noise measurement apparatus.

temperature ΔT_N with bias voltage. Using this synchronous technique, the signal-to-noise ratio is improved [19] by $\sqrt{B\tau}$, giving sensitivity of better than 5 mK in one second ($\tau = 1$) of integration.

Measurements of the shot noise spectrum were performed by rectifying the power in each channel with a diode. The diode outputs were fed to lock-in amplifiers, and the synchronous change in noise ΔT_N was detected for a 1 kHz square-wave modulation of the bias by $\pm 30 \mu\text{V}$ (60 μV p.p.). The lock-in readings were then recorded for a range of dc bias voltages, and the LO frequency for the high frequency channel was changed and the measurement repeated. The measurement technique is self-calibrating in the following sense: The amplifier noise is effectively subtracted by the lock-in amplifiers, leaving only one unknown parameter, the frequency-dependent gain of the system (in volts at the lock-in output per mK of device output noise). We expect that for large bias voltages such that $eV \gg kT$ and $h\nu$, the slope of noise temperature vs voltage should be the same for all frequencies and given by $S_I = 2eI/3$. Making this assumption, we can then scale the lock-in output for each frequency and compare the dependences on bias voltage, temperature, and frequency. An absolute calibration of the gain, and therefore, an accurate determination of the 1/3 suppression factor, was not possible in this configuration [20], as the amplifier noise drifts on the order of 1% over a few minutes.

The differential noise signals theoretically expected for the diffusive conductor, under the example conditions of 25 mK, all $D_n \ll 1$, and a small (30 μV p.p.) voltage modulation, are shown in the bottom of Fig. 1. If some of the D_n are not small, then the shot noise suppression simply multiplies the *differential* curves by an overall vertical scale factor of 1/3, but does not affect their *shape*. In particular, the cutoff voltage should be unaffected. The measured values of ΔT_N for frequencies of 1.5, 5, 10, 15, and 20 GHz, taken at a mixing chamber temperature of 40 mK, are shown in Fig. 3. While we see that ΔT_N for the low-frequency noise (circles) changes rapidly with voltage, approaching its linear asymptote at voltages of only a few times $kT/e \sim 10 \mu\text{V}$, the curves become successively broader for increasing frequencies. The noise for the highest frequencies has a clearly different shape, displaying the expected plateau for $|V| < V_{\text{cutoff}} = h\nu/e$ (about 80 μV for 20 GHz). Also shown in Fig. 3 (full lines) are theoretical curves based on Eq. (1), accounting for the finite voltage difference used, and for an electron temperature of 100 mK [21]. The asymptotic value of ΔT_N has been *arbitrarily scaled* (since the frequency-dependent system gain is not known to better than about 30%) to be 112 mK for each frequency, corresponding to the expected suppression factor of 1/3.

One potential source of systematic errors when detecting such small changes in noise power is a variation in the amplifier noise due to a bias-dependent change in the device impedance. Because of the extremely large bandwidth required, we could not use a microwave isolator between the

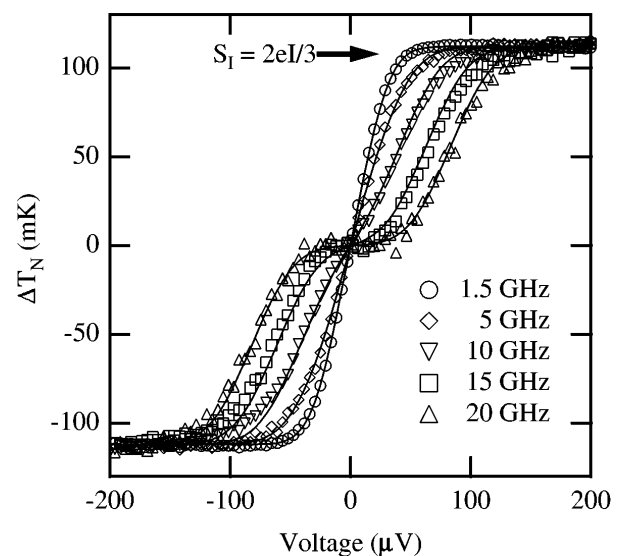


FIG. 3. Measured differential noise for frequencies of 1.5, 5, 10, 15, and 20 GHz, with mixing chamber temperature of 40 mK. Solid lines show the predictions of Eq. (1) for an electron temperature of 100 mK, and accounting for the voltage modulation of 60 μV p.p.

amplifier and sample. However, the sample impedance of 46.5 Ω is well matched to the amplifier and independent of bias voltage. Any frequency-dependent mismatch should simply cause a bias-independent change in the gain, and is automatically corrected via the technique described above. The critical conclusion of Fig. 3 relies on the systematic changes with frequency of the *shapes* of the ΔT_N curves vs bias voltage. Further proof that the observed shot noise cutoff must be due to vacuum fluctuations is obtained by measuring the ΔT_N curves at different temperatures. The data for two frequencies (1.5 and 20 GHz) and mixing chamber temperatures of 50 and 750 mK are compared in Fig. 4. The horizontal axes have been scaled to dimensionless units of eV/kT . As expected, at 750 mK, $h\nu/kT$ becomes small even for 20 GHz, and the data follow the same shape as the 1.5 GHz curves, which show only thermal broadening. Thus the cutoff in the shot noise, seen in the horizontal plateau of ΔT_N at 20 GHz and 50 mK, appears only in the quantum regime $h\nu \gg kT$, in agreement with Eq. (1).

Steinbach *et al.* [9] showed the existence of a “self-heating” regime for devices of intermediate length $L_{ee} < L < L_{eph}$. This also results in a linear increase in noise with large bias voltages, but with a slightly different slope from the suppressed shot noise, Eq. (1). Although we cannot distinguish these regimes by their slopes (since our overall system gain is not sufficiently well determined), we can differentiate between heating and shot noise by examining the *shape* of the low-frequency data vs voltage. The data for 1.5 GHz and a mixing chamber temperature of 750 mK are shown in the inset of Fig. 4, along with the best fits to the shot noise theory, Eq. (1) (full line), and the electron-heating theory (dotted line) given in [9]. The broadening observed is significantly *less* than that expected

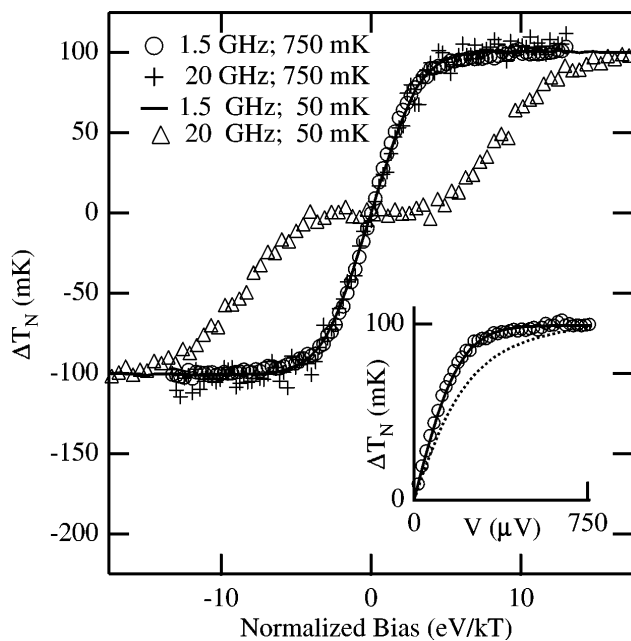


FIG. 4. Variation of differential noise ΔT_N with temperature. The differential noise at 1.5 GHz (full line) and 20 GHz (triangles), for a mixing chamber temperature of 50 mK, are plotted vs the dimensionless voltage in units of kT , along with corresponding data for 750 mK (circles and crosses, respectively). Inset shows a comparison of 1.5 GHz data for 750 mK with shot noise theory [full line, Eq. (1)] and electron-heating theory (dotted line).

for the electron heating, but in good agreement with shot noise. This agreement, taken in combination with the dependence on frequency of Fig. 3, provides conclusive proof that our sample is in the mesoscopic regime, and that the nonequilibrium fluctuations are due to shot noise, rather than electron heating within the sample.

The ability to perform “shot-noise spectroscopy” on mesoscopic devices should allow investigation of several other aspects of the dynamics of correlated electron transport in these systems. For example, Coulomb repulsions of the electrons in a 1- d conducting channel are predicted under certain conditions [22] to cause truly periodic oscillations at the frequency $f = I/e = (Ve^2/h)/e = eV/h$, which is the same as the cutoff frequency observed here. The spectrum given in Eq. (1) does not include Coulomb interactions, energy-dependent transmission coefficients, nor the finite transit time of electrons through the device. For a diffusive conductor, this last time scale is given by $\tau = L^2/D$ (or $\nu = 1/2\pi\tau \sim 16$ GHz for the device studied here) and can be made comparable to the inverse of the measurement frequency. Sensitive measurements of the noise can also reveal new effects which are not present in conductance. One example of these is the two-particle interference effect [14,23] which is visible only through studies of the noise in the presence of a time-varying Aharonov-Bohm flux.

In summary, we have measured the spectrum of the nonequilibrium current fluctuations of a diffusive meso-

scopic conductor in the high-frequency regime, where $h\nu \gg eV$ and kT . These measurements show the effects of vacuum fluctuations, which lead to a cutoff in the shot noise at a frequency $\nu_{\text{cutoff}} = eV/h$, in good agreement with the predicted spectrum for a quantum conductor [10,11].

The authors wish to acknowledge K. Segall, R. Zieve, and M. Deshpande for assistance with early experiments; and M. Reznikov, J.M. Martinis, A.H. Steinbach, L.S. Levitov, K.K. Likharev, B. Yurke, Y. Yamamoto, and R.G. Wheeler for useful discussions. This work was supported by NSF Grants No. DMR-9216121 and No. AST-9320387.

- [1] A. van der Ziel, *Noise in Solid State Devices and Circuits* (Wiley, New York, 1986).
- [2] Y.P. Li *et al.*, *Appl. Phys. Lett.* **57**, 774 (1990).
- [3] M. Reznikov *et al.*, *Phys. Rev. Lett.* **75**, 3340 (1995).
- [4] A. Kumar *et al.*, *Phys. Rev. Lett.* **76**, 2778 (1996).
- [5] V. A. Khlus, *Sov. Phys. JETP* **66**, 1243 (1987).
- [6] G. B. Lesovik, *JETP Lett.* **49**, 592 (1989).
- [7] C. W. J. Beenakker and M. Büttiker, *Phys. Rev. B* **46**, 1889 (1992).
- [8] M.J.M. de Jong, Ph.D. thesis, University of Leiden, the Netherlands.
- [9] A. H. Steinbach, J.M. Martinis, and M. H. Devoret, *Phys. Rev. Lett.* **76**, 3806 (1996).
- [10] S. E. Yang, *Solid State Commun.* **81**, 375 (1992).
- [11] M. Büttiker, *Phys. Rev. B* **45**, 3807 (1992).
- [12] A. J. Dahm *et al.*, *Phys. Rev. Lett.* **22**, 1416 (1969); D. Rogovin and D. J. Scalpino, *Ann. Phys.* **86**, 1 (1974).
- [13] H. B. Callen and T. A. Welton, *Phys. Rev.* **83**, 34 (1951).
- [14] G. B. Lesovik and L. S. Levitov, *Phys. Rev. Lett.* **72**, 538 (1994).
- [15] R. H. Koch, D. J. Van Harlingen, and J. Clarke, *Phys. Rev. Lett.* **47**, 1216 (1981).
- [16] R. Movshovich *et al.*, *Phys. Rev. Lett.* **65**, 1419 (1990); R. Movshovich *et al.*, *IEEE Trans. Magn.* **27**, 2658 (1991).
- [17] C. A. Mears *et al.*, *Appl. Phys. Lett.* **57**, 2487 (1990).
- [18] S. Wind *et al.*, *Phys. Rev. Lett.* **57**, 663 (1986).
- [19] R. H. Dicke, *Rev. Sci. Instrum.* **17**, 268 (1946).
- [20] Absolute calibrations could be performed in a separate experiment using a more sensitive, narrower-band amplifier at 1.5 GHz, via a Johnson noise thermometry technique. These results will be reported elsewhere, but showed suppression consistent with the expected 1/3 factor.
- [21] While care was taken to ensure good heat sinking of the leads and reduction of external heat sources, the effective electron temperature (~ 100 mK) is larger than the mixing chamber temperature of 40 mK, because of the finite thermal conductivity of the *macroscopic* contacts. For example, a Wiedemann-Franz thermal impedance equivalent to a lead resistance of only about 0.5Ω could account for the increase, due to the large (100 μV) biases applied.
- [22] D. V. Averin and K. K. Likharev, in *Nanostructures and Mesoscopic Systems*, edited by W. P. Kirk and M. A. Reed (Academic Press, Boston, 1992); D. V. Averin and Yu. V. Nazarov, *Phys. Rev. B* **49**, 2951 (1994).
- [23] L. Kouwenhoven, *Science* **271**, 1689 (1996).